ISSN : 0974-7419 Volume 10 Issue 12

Trade Science Inc.

Analytical CHEMISTRY

An Indian Journal

Full Paper

ACAIJ, 10(12), 2011 [817-824]

Mechanism studies on the interaction of Gemini surfactant 12-6-12 with bovine serum albumin by fluorescence method

Mengyao Hu, Xue Wang, Ling Li, Yu He, Gongwu Song*

Ministry-of-Education Key Laboratory for the Synthesis and Application of Organic Function Molecules, Hubei University, Wuhan 430062, P. R. (CHINA)

E -mail : songgw@hubu.edu.cn

Received: 7th July, 2011 ; Accepted: 7th August, 2011

ABSTRACT

The mechanism of the interaction between hexamethylene-1, 3-bis (dodecyldimethylammonium bromide) (Gemini 12-6-12) and bovine serum albumin was investigated by fluorescence spectroscopy. The results showed that the fluorescence quenching of BSA by 12-6-12 was attribute to the formation of the 12-6-12–BSA complex. Site marker competitive experiments demonstrated that the binding of 12-6-12 to BSA primarily took place in site I of BSA. The enthalpy change (ΔH) and entropy change (ΔS) were calculated to indicate that hydrophobic forces and hydrogen bond were the dominant intermolecular force in stabilizing the complex. Steady-state fluorescence indicates the strong interation between surfactant and BSA when the concentration of 12-6-12 is higher than the critical micelle concentration. The effect of 12-6-12 on the conformation of BSA was also analyzed by synchronous fluorescence spectrometry and TEM.

KEYWORDS

Gemini surfactant;
Bovine serum albumin;
Fluorescence;
Binding site.

INTRODUCTION

Proteins could bind many surfactants in vitro and in vivo to form a protein-surfactant complex where the hydrophobic moieties of the surfactant cause protein unfolding by interacting with the nonpolar amino acid residues[1-6]. Understanding their interaction mechanism is not only of fundamental interest in life science, but of practical importance in industrial application. For instant, in the field of pharmaceutics, paints, adhesives and oil recovery, protein function is significantly influenced by the addition of surfactant[7-10]. And these interaction mechanisms are important to understand the action of surfactants as solubilizing agents to recover proteins from inclusion bodies and in the renaturation of the proteins produced in the genetically engineered cells via the artificial chaperone protocol[11-16].

Gemini surfactant molecule is a dimeric substance composed of two identical amphiphilic moieties covalently linked by a spacer group at or near the ionic headgroup[17]. Because of the hydrophobic and hydrophilic properties of the amino acids, a protein exhibits dualism that causes amphiphilic molecules to interact with it. Ionic surfactants was chosen for the study of protein-surfactant interactions for their application in the area of membrane study[18, 19]. The interaction between cationic surfactants and proteins was seldom reported compared to the anionic surfactants since the ionic sur-

factants bound to the oppositely charged sites of protein structure at the neutral pH values[20]. Herein, the research of protein-gemini surfactants provides immense information on the BSA-surfactant interaction process.

In this work, we investigate the interactions between bovine serum albumin (BSA) and cationic gemini surfactant hexamethylene - 1, 3 - bis (dodecyl dimethylammonium bromide) (12-6-12). The molecular structure of gemini sufactant 12-6-12 was shown in Figure 1. BSA usually functions as a carrier for fatty acid in bloodand for conjugation in antibody production. The primary structure of BSA consists of nine loops held together by 17 disulfide bonds, which results in three domains each containing two sub-domains or alternatively one small and two large loops[3, 21, 22]. These structures are important for molecules combining to BSA. We have employed fluorescence spectroscopy–based method and TEM measurements in order to obtain information related to the binding mechanisms between the surfactants and BSA such as binding modes, binding constants, binding sites and quenching rate constants.

Figure 1 : Molecular structure of Gemini surfactant 12-6-12

EXPERIMENTAL

Reagents

Gemini 12-6-12, BSA, warfarin and ibuprofen were obtained from Hubei University, Wuhan Tianyuan Biotechnology Co. Ltd. and Wuhan Kaibo Instruments Co. Ltd., respectively. Pyrene (Py) (Alfa Aesar) was dissolved in methanol and the prepared concentration was 1.05×10^{-6} mol L^{-1}. Chemicals were all of analytical grade and doubly distilled water was used throughout the experiment.

Fluorescence measurements

All fluorescence spectra were measured on an RF-540 fluorophotometer (Tokyo, Japan) equipped with a 1.0 cm quartz cell and a thermostat bath. In a typical fluorescence measurement, BSA(3.0 mL, 2.0×10^{-6} mol L^{-1}) was added into the quartz cell and then titrated by various concentration of 12-6-12. Titrations operated manually and mixed moderately.

The fluorescence emission spectra were measured at 293, 298 and 303 K, respectively. An excitation wavelength of 280 nm was chosen and the emission wavelength was recorded from 290 to 450 nm.

Site marker competitive experiments

Binding location studies between 12-6-12 and BSA in the presence of two sitemarkers (warfarin and ibuprofen) were measured using the fluorescence titration methods. The concentrations of BSA and warfarin/ibuprofen were all stabilized at 2.0×10^{-6} mol L^{-1}. 12-6-12 was then gradually added to the BSA–warfarin or BSA–ibuprofen mixtures. An excitation wavelength of 280nm was selected and the fluorescence spectra were recorded from 290–450 nm.

RESULTS AND DISCUSSION

Interactions between 12-6-12 and BSA

Figure 2 showed the fluorescence emission spectra of BSA at different concentrations of 12-6-12. When different amount 12-6-12 was titrated into a fixed concentration of BSA, the fluorescence intensity of BSA at around 350 nm decreased regularly and the emission peak was shift to shorter wavelength, which indicated some change in the local dielectric environment of BSA.

Fluorescence quenching mechanisms are usually classified as either dynamic or static quenching, which can be distinguished by their different dependence on temperature or viscosity, or preferably by lifetime measurements[23, 24]. For static quenching, the quenching constants decrease with the increased temperature, while the reverse effect is observed for the case of dynamic quenching. In order to Figure out which mechanism play a dominant role in the interaction, the fluorescence quenching process is firstly assumed to be a dynamic mechanism. For dynamic quenching, the decrease in intensity is usually analyzed using the Stern–Volmer equation[24]:

$$\frac{F_0}{F} = 1 + k_q\tau_0[Q] = 1 + K_{SV}[Q] \quad (1)$$

where F_0 and F are the fluorescence intensities in the absence and presence of the quencher, respectively; K_{SV} is the Stern–Volmer quenching constant; $[Q]$ is the concentration of the quencher; τ_0 is the average fluo-

rescence lifetime of bimolecular and equal to 10^{-8} s[25]; k_q, which is equal to K_{SV}/τ_0 is the apparent bimolecular quenching rate constant. For dynamic quenching, the maximum scattering collisional quenching constant of various quenchers is 2.0×10^{10} L mol^{-1} s^{-1}[26].

Figure 3 showed the influence about $[F_0/F\text{-}Q]$ at different temperature, and TABLE 1 presented the calculated K_{SV} and k_q at each temperature. The results showed that the Stern–Volmer quenching constants K_{SV} decreased with the increase of temperature and the values of k_q were much larger than 2.0×10^{10} L mol^{-1} s^{-1}. As a result, the probable quenching mechanism of the intrinsic fluorescence of BSA was not initiated by a dynamic process, but resulted from a complex formation between BSA and 12-6-12. Meanwhile, it was found that the values of K_{SV} were all great; the reason might be that the fluorescent quantum yield of BSA increased or a strong binding existed between BSA and 12-6-12[27].

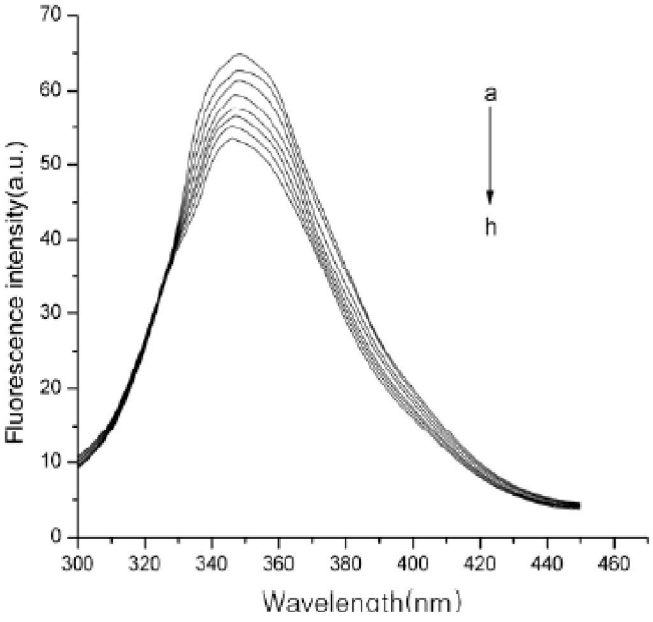

Figure 2 : Emission spectra of BSA at different concentrations of 12-6-12 (T = 293K and λ_{ex} = 280 nm). C_{BSA} = 2.0×10^{-6} mol L^{-1}; $C_{12\text{-}6\text{-}12}$ =2×10^{-4} mol L^{-1}, a–h: 0, 5, 10, 15, 20,25, 30, 35 µL, respectively.

TABLE 1 : Stern–Volmer quenching constants for the interaction of 12-6-12 with BSA at different temeratures.

T(K)	K_{SV}($\times10^4$ Lmol$^{?1}$)	kq ($\times10^{12}$ Lmol$^{?1}$ s$^{?1}$)	R
293	8.9908	8.9908	0.9987
298	2.3284	2.3284	0.9857
303	1.4892	1.4892	0.9689

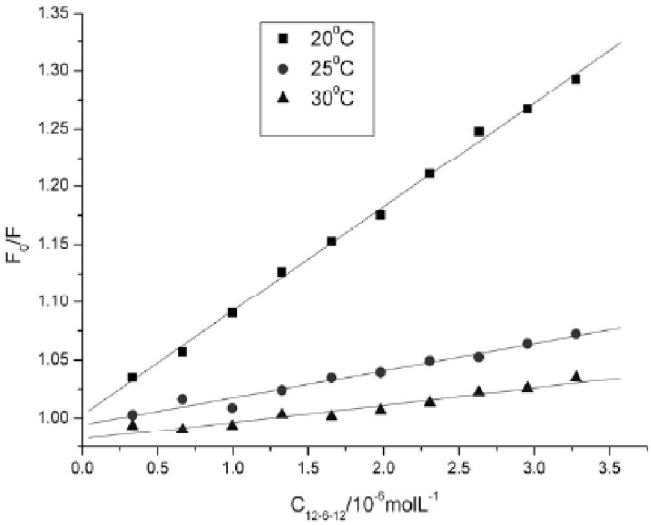

Figure 3 : Emission spectra of BSA with various concentrations of 12-6-12 at different temperature C_{BSA} = 2.0×10^{-6} mol L^{-1}; $C_{12\text{-}6\text{-}12}$ =2×10^{-4} mol L^{-1}

Number of binding sites and identification of the binding location of 12-6-12 on BSA

As discussed above, 12-6-12-induced fluorescence quenching of BSA was a static quenching process. Florescence quenching data of BSA were analyzed to obtain various binding parameters. The binding constant (K_b) and the number of binding sites (n) can be calculated according to the equation[28]:

$$\log[\frac{F_0 - F}{F}] = \log K + n\log[Q] \qquad (2)$$

where F_0 and F are the fluorescence intensity without and with the ligand, respectively. Aplot of log [(F_0 - F)/F] vs. log [Q] gave a straight line using least squares analysis whose slope was equal to n (binding sites) and the intercept on Y-axis to log K (K equal to the binding constant). From Eq.(5), the values of K and n at 293K were obtained to be 5.531×10^4 L mol^{-1} and 0.9618 respectively, which implied that 12-6-12 bound strongly to BSA and there was one independent class of binding sites for 12-6-12 towards BSA. The linear coefficient R (0.9976) indicated that the assumptions underlying the derivation of Eq. (5) were satisfactory.

Crystal structure of BSA shows that BSA is a heart-shaped helical monomer composed of three homologous domains named I–III, and each domain includes two sub-domains called A and B to form a cylinder[29]. According to Refs.[30,31], the principal regions of ligands bound to BSA are usually located in hydrophobic cavi-

ties in sub-domains IIA and IIIA, and the binging cavities associated with sub-domains IIA and IIIA are also referred to as sites I and II. As the data in the preceding discussion did not allow us to give the precise binding location of 12-6-12 on BSA, the sitemarker competitive experiments were then carried out, using drugs which specifically bind to a known site or region on BSA. As described in the literature, warfarin has been demonstrated to bind to the sub-domain IIA while ibuprofen is considered as sub-domain IIIA binder[32]. By monitoring the changes in the fluorescence intensity of 12-6-12 bound BSA that brought about by site I (warfarin) and site II (ibuprofen) markers, information about the specific binding site of 12-6-12 in BSA can be gained.

In order to compare the effect of warfarin and ibuprofen on the binding of 12-6-12 to BSA, the fluorescence quenching data BSA with the presence of site markers were also analyzed using the Stern–Volmer equation, as shown in Figure 4. The binding constants of the systems, which can be calculated from the slope values of the plots, were listed in TABLE 2. Obviously, the *K* values of the system with warfarin were almost 67.8% of that without warfarin, while the constants of the systems with and without ibuprofen had nearly no difference. It indicated that there was a significant competition between 12-6-12 and warfarin, while ibuprofen had neaely no influence on the binding of 12-6-12 to BSA. The above experimental results and analysis demonstrated that the binding of 12-6-12 to BSA mainly located within site I (sub-domain IIA)

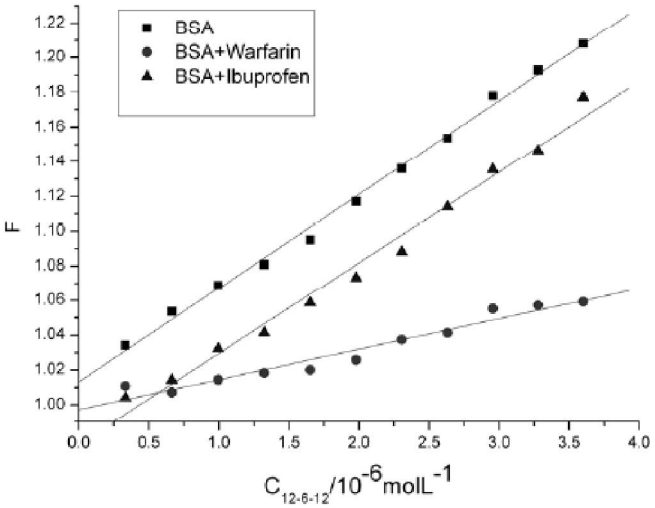

Figure 4 : Stern–Volmer plots for the 12-6-12–BSA system in the absence and presence of site markers (*T* = 293K)

TABLE 2 : The binding constants of competitive experiments of 12-6-12–BSA system.

Site market	K_a ($\times 10^4$ L mol$^{?1}$)	*R*
Blank	5.3987	0.9978
Ibuprofen	5.2211	0.9744
Warfarin	1.7382	0.9928

Determination of the force acting between 12-6-12 and BSA

Essentially, the interaction forces between ligands and biological macromolecules may include hydrophobic force, multiple hydrogen bond, Van der Waals force and electrostatic interactions[33]. The signs and magnitudes of the thermodynamic parameters (ΔH and ΔS) can account for the main forces involved in the binding process. For this reason, the temperature-dependent binding constantwas studied. The temperatures chosenwere 293, 298 and 303K, thus BSA would not undergo any structural degradation. If the enthalpy change (ΔH) does not vary significantly in the temperature range studied, both the enthalpy change (ΔH) and entropy change (ΔS) can be evaluated from the van't Hoff equation:

$$\ln(\frac{k_2}{k_1}) = \frac{(\frac{1}{T_1} - \frac{1}{T_2})}{R}\Delta H \quad (3)$$

k_1 and k_2 are the binding constant at different temperature and R is the gas constant. The enthalpy change (ΔH) could be calculated from the slope of the van't Hoff plot. The free energy change (ΔG) was then estimated from the following relationship:

$$\Delta G = \Delta H - T\Delta S \quad (4)$$

$$\Delta G = -RT \ln K \quad (5)$$

TABLE 3 shows the values of ΔH, ΔG and ΔS in different temperature. As can be found from the values of ΔH (-66.68 kJmol^{-1}) and ΔS (136.79 Jmol^{-1} K^{-1}, 293K) that the binding process was mainly driven by the entropy change, the enthalpy change has little contribution. The negative value of ΔG revealed the binding process was spontaneous. Ross and Subramanian[34] have characterized the sign and magnitude of the thermodynamic parameter associated with various individual kinds of interaction that may take place in protein association process. From the point of view of water structure, a positive ΔS value is frequently taken as evidence

for a hydrophobic interaction because the water molecules are arranged in an orderly fashion around the surfactant and protein acquires a more random configuration[35]. A negative ΔH value is frequently taken as evidence for hydrogen bond in the binding interaction[36], and from the structure of 12-6-12, H-bond can be formed in the nitrogen atom. And the negative value of ΔH (–66.68 kJmol^{-1}) observed in this experiment cannot be attributed to electrostatic interactions, since the value of ΔH is very small[36]. Thus, from the thermodynamic characteristics summarized above, hydrophobic forces and hydrogen bond played major roles in the 12-6-12–BSA binding reaction and contributed to the stability of the complex.

TABLE 3 : The binding constant and relative thermodynamic parameters of the 12-6-12–BSA system

T(K)	K	R	ΔH(kJ mol$^{?1}$)	ΔG (kJ mol$^{?1}$)	ΔS(J mol$^{?1}$ K$^{?1}$)
293	5.531×10^4	0.9976	-66.68	-26.60	136.79
298	3.494×10^4	0.9922		-25.92	136.77

Micropolarity and micelle aggregation numbers (N)

After the research of the behavior of individual surfactant molecules ▪ Cwe should discuss the interaction between surfactant micelle and protein Pyrene has been widely used as a probe of interactions between surfactant and polymers[37, 38]. 10 µl Py stock solutions were added to the samples prepared by dilution of different 12-6-12 stock solutions. The typical emission spectrum of pyrene (λ_{EX}=335 nm) has five peaks at 373, 379, 384, 390, and 397 nm, and the ratio of the first to third vibronic peaks I_1/I_3 is used to detect the microenvironment of pyrene, being high in polar media and low in hydrophobic environments. Figure 5 showed the plots of I_1/I_3 for pyrene solubilized in different concentration of surfactant. When the solution concentration of 12-6-12 increased to a certain value, the curve abrupt change, and this concentration is defined as critical micelle concentration (cmc). The cmc value keeps almost constant at about 6.15×10^{-4} mol L^{-1}.

Turro had made the following assumptions: quenching rate is much greater than the decay rate of the probe. The fluorescence of all the probe would be quenched which contains quenchers in the micelles. By measuring the fluorescence emission spectrum of pyrene at 374nm in different concentration of quenchers, then the micelle aggregation numbers can be analyzed according the following formula[39]:

$$\ln(\frac{I_0}{I}) = N\frac{[Q]}{C_{\text{surfactant}} - cmc} \quad (6)$$

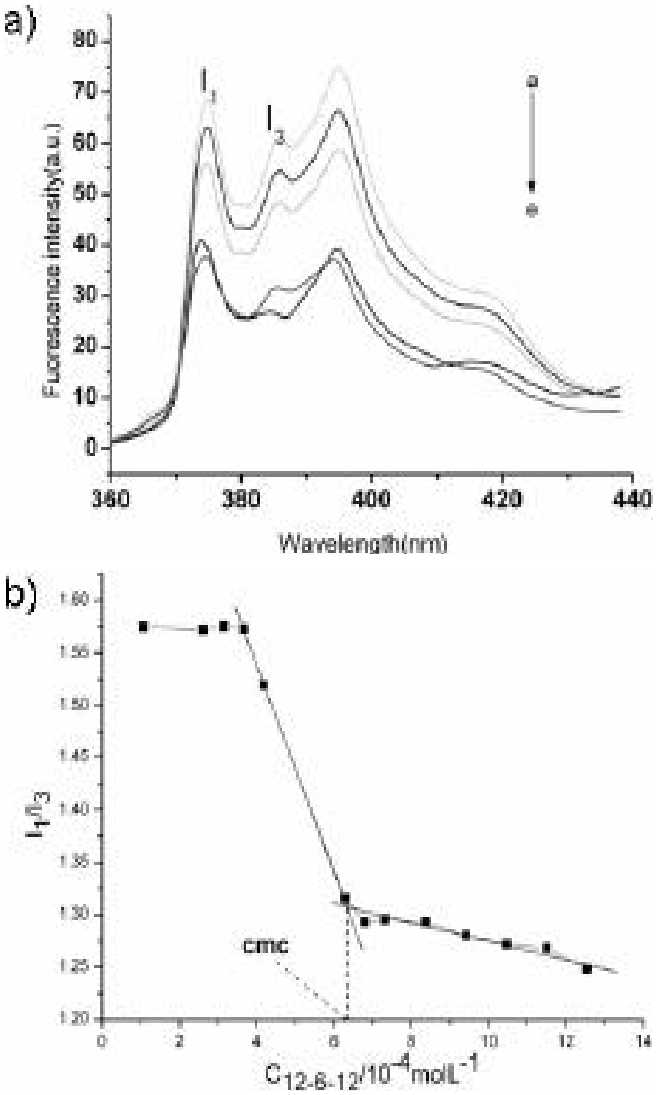

Figure 5 : Emission spectra of Py with various concentrations of 12-6-12 (a) CPy: 1.05×10-6 molL-1; C12-6-12£°0.0104 mol/L£»a-e£°0.1, 0.2, 0.3, 0.4, 0.5 (b) Dependence of I1/I3 on 12-6-12 concentration

TABLE 4 : The micelle aggregation numbers (N) of different 12-6-12-BSA system

	C_{BSA}(mol L^{-1})	N	R
12-6-12(5cmc)	0 molL^{-1}	12.95	0.9985
12-6-12(5cmc)+BSA	8.33×10^{-7}molL^{-1}	10.96	0.9969
12-6-12(5cmc)+BSA	1.67×10^{-6}molL^{-1}	10.47	0.9991

Full Paper

where I_{0375} and I_{375} are the fluorescence intensity without and with the quencher at 375 nm. [*Q*] is the concentration of the quencher; $C_{surfactant}$ is the concentration of the surfactant; cmc is the critical micelle concentration of 12-6-12 at that condition. A plot of log [I_0 / I] vs. [Q / $C_{surfactant}$ - cmc] gave a straight line using least squares analysis whose slope was equal to *N*. And TABLE 4 showed the N value of 12-6-12 at fivefold cmc with different concentration of BSA. The N value of the Py/surfacant/BSA system is smaller than that of Py/surfactant system, which indicated that the 12-6-12 could be transferred from the micelle by interacting with BSA. The phenomena proved the strong binding between 12-6-12 and BSA.

Synchronous spectra

Synchronous fluorescence spectra of BSA were shown in Figure 6. The fluorescence intensity of BSA for $\Delta\lambda$ =60 nm is higher than that for $\Delta\lambda$ =20 nm, indicating that the fluorescence peak at 347 nm should be mainly contributed by tryptophan. On the other hand, the fluorescence intensity of BSA decreased for $\Delta\lambda$ =60 nm and increases for $\Delta\lambda$ = 20 nm when 12-6-12 was added. However, the decrease of the fluorescence intensity for $\Delta\lambda$ =60 nm was much larger than the increase for $\Delta\lambda$ =20 nm at the same concentration of 12-6-12. Therefore, 12-6-12 mainly interacts with tryptophan residues and this conclusion was also found in 12-6-12/BSA system

TEM micrographs of surfactants binding to BSA

Figure 7 exhibited the TEM images of 12-6-12 Gemini surfactants before and after binding to BSA. Figure 7a shows the monomer of 12-6-12 is "spherical" molecule with diameter of 20 nm. The TEM of 12-6-12/BSA nanocomposites showed that the aggregation between 12-6-12 and BSA was formed with diameter of 500 nm (Figure 7b).

CONCLUSIONS

The interaction mechanism between gemini surfactant 12-6-12 and BSA was investigated using fluorescence spectroscopy–based method and TEM measurements. The fluorescence of BSA was quenched with a little blue shift indicating the formation of the

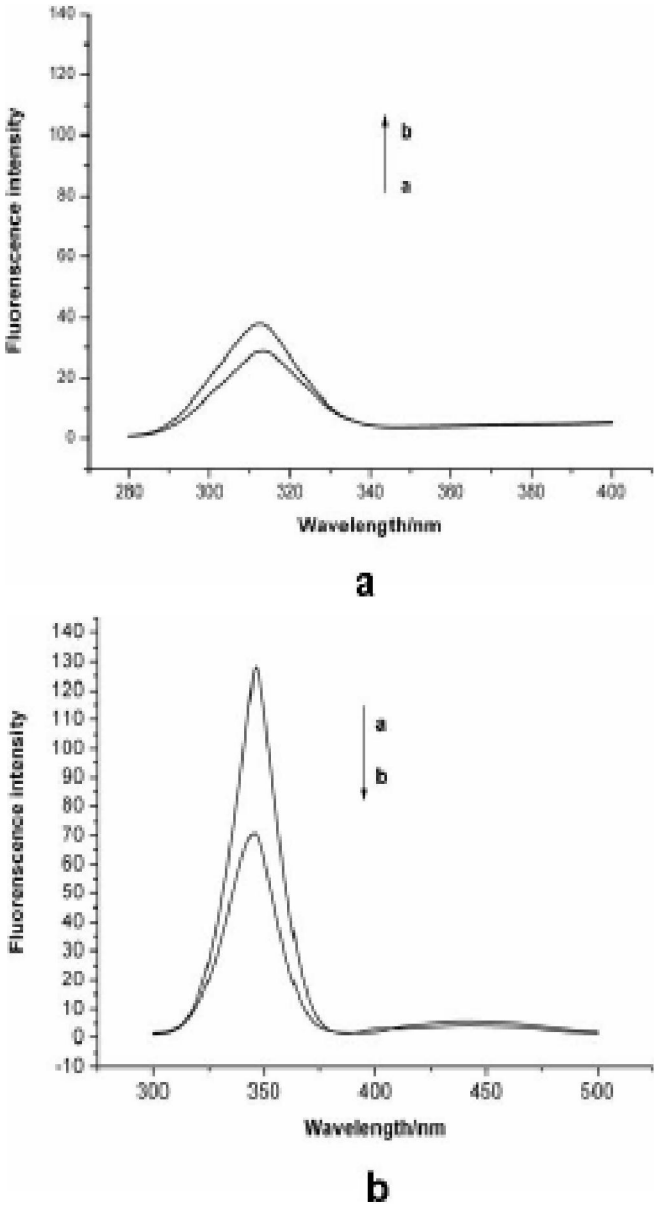

Figure 6 : Synchronous fluorescence spectrum of BSA: (A) $\Delta\lambda$=20nm; (B) $\Delta\lambda$=60nm; c_{BSA} = 1.0×10^{-6} mol L^{-1}, $C_{12\text{-}6\text{-}12}$ (×10^{-3} mol L^{-1}), a–b: 0, 1.6mL respectively.

nanocomposite between gemini surfactant 12-6-12 and BSA. The enthalpy change (ΔH) and entropy change (ΔS) were calculated to indicate that hydrophobic forces and hydrogen bond played major roles in the 12-6-12–BSA binding reaction and contributed to the stability of the complex Site marker competitive experiments showed that 14-6-14 bound to the sub-domain II A of BSA, which was the same as that of warfarin binding to BSA. Steady-state fluorescence and TEM measurements also can prove that strong binding between 12-6-12 and BSA.

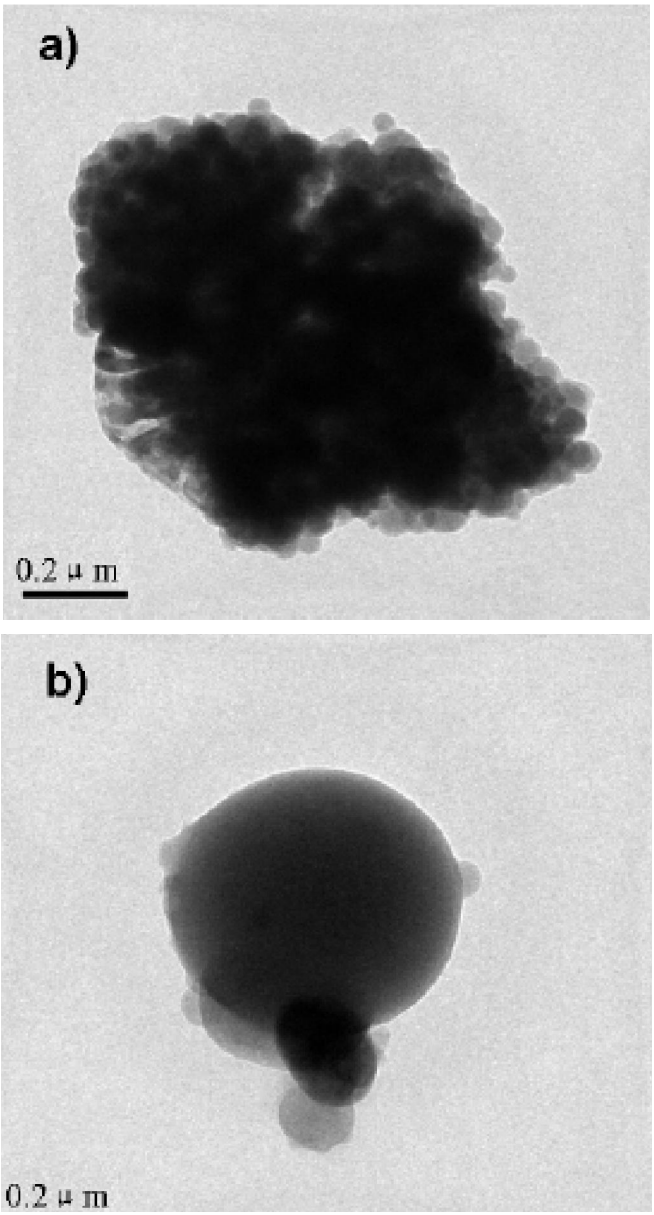

Figure 7 : TEM micrographs of surfactants (a) before and (b) after binding to BSA. $C_{12\text{-}6\text{-}12}=4.0\times10^{-4}$mol L^{-1}, $C_{BSA}=1.0\times10^{-6}$mol L^{-1}.

ACKNOWLADGEMENTS

This work was financially supported by the Scientific Research Foundation of Education Commission of Hubei Province (Q20111010 and T201101).

REFERENCES

[1] C.La Mesa; J.Colloid Interface Sci., **286**, 148-157 **(2005)**.
[2] S.Chodankar, V.K.Aswal, P.A.Hassan, A.G.Wagh; Phys.B., **398**, 112-117 **(2007)**.
[3] S.De, A.Girigoswami, S.Das; J.Colloid Interface Sci., **285**, 562-573 **(2005)**.
[4] C.T.Lee, K.A.Smith, T.A.Hatton; Biochemistry., **44**, 524-536 **(2005)**.
[5] C. Sun, J.Yang, X.Wu, X.Huang, F.Wang, S.Liu; Biophys.J., **88**, 3518-3524 **(2005)**.
[6] R.C.Lu, A.N.Cao, L.H.Lai, J.X.Xiao; Colloids Surf.A., **278**, 67-73 **(2006)**.
[7] K.P.Ananthapadmanabhan; In Interactions of Surfactants with Polymers and Proteins, E.D.Goddard, K.P.Ananthapadmanabhan, Eds, CRC Press, Inc: London, U.K., Chapter 8, **(1993)**.
[8] M.N.Jones; Chem.Soc.ReV., **21**, 127-136 **(1992)**.
[9] M.N.Jones; In Food Polymers, Gels and Colloids; Dickenson, E., Ed., The Royal Society of Chemistry: Cambridge, U.K. 65-80, **(1991)**.
[10] D.J.McClements; Food Emulsions: Principles, Practice and Techniques, 2nd Edition, CRC Press: Boca Raton, FL., **(2004)**.
[11] B.P.Kamat, J.Seetharamappa; J.Pharm.Biomed.Anal., **35**, 655-664 **(2004)**.
[12] F.Khodagholi, B.Eftekharzadeh, R.Yazdanparast; Protein J., **27**, 123-129 **(2008)**.
[13] A.Sulkowska; J.Mol.Struct., **614**, 227-232 **(2002)**.
[14] D.Kelley, D.J.McClements; Food Hydrocolloids., **17**, 73-85 **(2003)**.
[15] C.Sun, J.Yang, X.Wu, X.Huang, F.Wang, S.Liu; Biophys.J., **88**, 3518-3524 **(2005)**.
[16] Y.Koichi, O.Masato, M.Haruo; Analytica Chimica Acta., **455**, 83-92 **(2002)**.
[17] D.C.Carter, J.X.Ho; Adv.Prot.Chem., **45**, 153-203 **(1994)**.
[18] S.Matysik, F.M.Matysik, W.D.Einicke; Sensors and Actuators B: Chemical **85**, 104-108 **(2002)**.
[19] A.V.Few, R.H.Ottewill, H.C.Parreira; Biochim.Biophys., **18**, 136-137 **(1955)**.
[20] F.Menger, C.A.Littau; J.Am.Chem.Soc., **115**, 10083-10090 **(1993)**.
[21] J.R.Brown; In Albumin Structure, Function, and Uses; Rosenoer, V. M.; Oratz, M.; Rothschild, M. A. Eds., Pergamon Press: Oxford 27-51, **(1977)**.
[22] T.J.Peters; In All About Albumin. Biochemistry, Genetics and Medical Applications; San Diego: Academic Press 9-75, **(1996)**.
[23] B.Ahmad, S.Parveen, R.H.Khan; Biomacromolecules., **7**, 1350-1356 **(2006)**.
[24] J.R.Lakowicz; Principles of Fluorescence Spectroscopy, 2nd Edition, Plenum Press, New York, **(1999)**.
[25] J.R.Lakowicz, G.Weber; Biochemistry., **12**, 4161-

4170 **(1973)**.
[26] W.R.Ware; J.Phys.Chem., **66**, 455-458 **(1962)**.
[27] H.Xu, Q.W.Liu, Y.Q.Wen; Spectrochim. Acta Part A: Mol.Biomol.Spectrosc., **71**, 984-988 **(2008)**.
[28] J.Kang, Y.Liu, M.X.Xie, S.Li, M.Jiang, Y.D.Wang; Biochim.Biophys.Acta., **1674**, 205-214 **(2004)**.
[29] U.Kragh-Hansen; Pharm.Rev., **33**, 17-53 **(1981)**.
[30] G.Sudlow, D.J.Birkett, D.N.Wade; Mol.Pharmacol., **11**, 824-832 **(1975)**.
[31] P.B.Kandagal, S.M.T.Shaikh, D.H.Manjunatha, J.Seetharamappa, B.S.Nagaralli; J.Photochem.Photobiol.A., **189**, 121-127 **(2007)**.
[32] X.M.He, D.C.Carter; Nature., **358**, 209-215 **(1992)**.
[33] D.Leckband; Annu.Rev.Biophys.Biomol.Struct., **29**, 1-26 **(2000)**.
[34] P.D.Ross, S.Subramanian; Biochemistry., **20**, 3096-3102 **(1981)**.
[35] D.J.Li, J.F.Zhu, J.Jin, X.J.Yao; J.Mol.Struct., **846**, 34-41 **(2007)**.
[36] M.H.Rahman, T.Maruyama, T.Okada, K.Yamasaki, M.Otagiri; Biochem.Pharmacol., **46**, 1721-1731 **(1993)**.
[37] P.Hansson; Langmuir., **17**, 4161-4166 **(2001)**.
[38] A.Hashidzume, M.Mizusaki, K.Yoda, Y.Morishima; Langmuir., **15**, 4276-4282 **(1999)**.
[39] X.G.Wang, F.Yan, C.R.Zhang; Photographic Science and Photochemistry., **25**, 32-39 **(2007)**.